Model Reduction for Heat Grid State Estimation

Andreas Bott [1], Pascal Friedrich [2], Lea Rehlich [3], Florian Steinke [1]
[1] *Energy Information Networks & Systems*, [2] *Multi-Modal Energy Systems*, [3] *Research Group Optimization*
Technische Universität Darmstadt, Germany
{andreas.bott@eins., pascal.friedrich@mmes., rehlich@mathematik., florian.steinke@eins.}@tu-darmstadt.de

***Abstract*—Traditional district heating networks have been built around few central heat production units. Now, many more decentral heat sources based on renewable energies or waste heat are being included to reduce carbon emissions. Given the resulting complex flow patterns in the network reliable and fast heat grid state estimation becomes mandatory for efficient grid control. In this paper we first show an approach to reduce computational efforts for various grid computations by summarising pipe segments of the network. We then develop a probabilistic state estimator based on the reduced model by locally linearising the non-linear grid equations around the best state estimate. We show that the linearisation approach with a significantly lower computational burden achieves a prediction quality comparable to those of a sampling-based Monte-Carlo approach that uses the full model. This allows state estimation to become an online routine even in complex heating networks.**

***Index Terms*—district heating, model reduction, state estimation**

I. INTRODUCTION

For reducing carbon emissions in district heating the transformation of traditional heating networks with few large suppliers into 4th generation networks is required [1]. These are characterised by decentralised suppliers as well as low temperature levels. Therefore, traditional control strategies are replaced by new methods based on heat grid state estimation.

Steady state heat grid models are commonly used for analysing different aspects of district heating networks as well as for state estimation, for example, in [2]–[6]. In contrast to electrical power networks, however, the question of probabilistic state estimation is scarcely addressed in this context. One approach on this topic is given in [6] by locally accumulating uncertainties in treelike networks. In this paper, we propose an approach to probabilistic state estimation using a global linearisation of the steady state equations. This approach allows the incorporation of the correlation structure among consumer demands. Furthermore it can be expanded for networks which are not treelike or have multiple heat producers. A potential downside to our approach is that the non-linear state equations have to be solved and local derivatives have to be calculated. This represents a significant computational effort. In order to minimise this effort, we apply a model reduction method by summarising similar line segments. Summarisation has been proposed by [7], [8], [9]. However, we only merge serial network components and therefore retain the full customer and supplier structure. We thus choose a middle way between full resolution of the network topology and the merging of whole network sections. Moreover, we simplify the computationally expensive equations describing pressure losses in the network, similar to [10]. All model reduction steps are carefully examined for their accuracy.

In Section II, we first introduce the steady-state model equations for heating grids which are the basis of the state estimation algorithm. An approach to reduce the complexity of various grids by simplifying the network structure is shown in Section III and the linearisation step is described in Section IV. In Section V we provide experimental results for a slightly modified subset of a real district heating network. We conclude in Section VI.

This research was funded by the German Federal Ministry for economic affairs and energy (BMWi) – project number 03EN3012A

II. HEAT MODEL EQUATIONS

The network state in heating grids is determined by the heat extracted by the consumers and the set points for pressure and temperature at the heating plants. To ensure the security of supply these set points have to be adjusted according to the demand. The heating network can be represented as a graph $\boldsymbol{G} = (\boldsymbol{V}, \boldsymbol{E})$ with nodes $\boldsymbol{V}$ and edges $\boldsymbol{E} \subseteq \boldsymbol{V} \times \boldsymbol{V}$. The network state is defined by the pressures p_i and the temperatures T_i at nodes i, as well as the water temperatures at the end T_{kl}^{end} and the start T_{kl}^{start} of each edge $(k,l) \in \boldsymbol{E}$. The mass flow rate through edge (k,l) is denoted by $\dot{m}_{kl}$. For each edge $(k,l) \in \boldsymbol{E}$ we define the nominal flow direction from k to l such that $\dot{m}_{kl}$ is positive if mass flows from node k towards node l and negative if mass flows from node l towards node k. Per definition it follows that $\dot{m}_{ij} = -\dot{m}_{ji}$ and $T_{ij}^{\mathrm{end}} = T_{ji}^{\mathrm{start}}$. We assume steady state conditions and neglect time delays in the network. Water is assumed to be incompressible with constant fluid properties.

Let $\boldsymbol{N}_i \coloneqq \{j \in \boldsymbol{V} \mid (i,j) \in \boldsymbol{E}\}$ be the set of all nodes that share an edge with i. According to the mass conservation, ingoing and outgoing flows at every node add up to zero,

$$\sum_{j \in \boldsymbol{N}_i} \dot{m}_{ij} = 0, \qquad \forall i \in \boldsymbol{V}\,. \tag{1}$$

Similarly the temperature in each node is determined by the mixing laws of thermodynamics,

$$T_i = \frac{\sum\limits_{j \in \boldsymbol{N}_i, \dot{m}_{ji} > 0} \dot{m}_{ji}\, T_{ji}^{\mathrm{end}}}{\sum\limits_{j \in \boldsymbol{N}_i, \dot{m}_{ji} > 0} \dot{m}_{ji}}, \ \forall i \in \boldsymbol{V}\,. \tag{2}$$

The temperature at the start of an edge $(i,j) \in \boldsymbol{E}$ is given by the temperature at node i if the mass flow goes from i to j,

$$T_{ij}^{\text{start}} = T_i, \quad \forall (i,j) \in \boldsymbol{E} \text{ with } \dot{m}_{ij} \geq 0. \tag{3}$$

We distinguish four types of edges, each characterised by the pressure change along the edge Δp_{ij} and the temperature at the end of the edge T_{ij}^{end}. For straight pipes $(i,j) \in \boldsymbol{E}^{pipe}$ the temperature loss depends on the ambient temperature T_a, the specific heat capacity of water c_p, as well as the heat energy loss coefficient λ_{ij} and the length l_{ij} of the pipe,

$$T_{ij}^{\text{end}} = \left(T_{ij}^{\text{start}} - T_{\text{a}}\right) \exp\left(-\frac{l_{ij}\lambda_{ij}}{c_p \dot{m}_{ij}}\right) + T_{\text{a}}\,. \tag{4}$$

The pressure loss in these pipes depends on the pipe diameter d_{ij}, the density of water ρ and the Darcy friction factor $f_{\text{D},ij}$,

$$\Delta p_{ij} = f_{\text{D},ij} \frac{8 l_{ij}}{\pi^2 \rho d_{ij}^5} \dot{m}_{ij} |\dot{m}_{ij}|, \ \forall (i,j) \in \boldsymbol{E}^{\text{pipe}}\,. \tag{5}$$

The Darcy friction factor $f_{\text{D},ij}$ is computed with the Colebrook-White equation which depends on the Reynolds number and needs to be solved numerically since it is formulated implicitly, cf. [11].

Additional pressure losses appear in bended pipes. These losses are incorporated by introducing bend edges $\boldsymbol{E}^{Bend}$ which have no physical extension. For these edges we use

$$T_{ij}^{\text{end}} = T_{ij}^{\text{start}}, \qquad \forall (i,j) \in \boldsymbol{E}^{bend}, \tag{6}$$

$$\Delta p_{ij} = \zeta_{ij} \frac{8}{\pi^2 \rho d_{ij}^4} \dot{m}_{ij} |\dot{m}_{ij}|, \qquad \forall (i,j) \in \boldsymbol{E}^{bend}\,. \tag{7}$$

The pressure loss thus depends on a loss factor ζ_{ij} which is approximated with the experimentally defined relations presented in [12]. The equations are defined piecewise depending, e.g., on the Reynolds number and the bending angle. For the existing non-defined regions we interpolate linearly.

Equations (1) - (7) describe the physical behaviours of the pipes in the network. Pressure losses due to mixing at junctions (e.g. T-fittings) are neglected. To fully define the network state we also need to specify the consumer and generator behaviour.

Consumer edges $\boldsymbol{E}^{demand}$ are modelled by a given demand $\dot{Q}_{ij}$ and a fixed return temperature T_{ij}^{set} [13]

$$T_{ij}^{\text{end}} = T_{ij}^{set}, \qquad \forall (i,j) \in \boldsymbol{E}^{demand}, \tag{8}$$

$$\dot{Q}_{ij} = \dot{m}_{ij} c_p \left(T_{ij}^{\text{start}} - T_{ij}^{\text{end}}\right), \quad \forall (i,j) \in \boldsymbol{E}^{demand}. \tag{9}$$

In the experiments of this paper, we consider one heat producer as a slack edge $\boldsymbol{E}^{heating}$, providing the necessary heating power as well as the pressure difference between the return and supply side. This is modelled by fixing the temperature T_{ij}^{end} to a given set point T_{ij}^{set},

$$T_{ij}^{\text{end}} = T_{ij}^{set}, \qquad \forall (i,j) \in \boldsymbol{E}^{heating}\,. \tag{10}$$

The pressure in the network is determined by the so-called worst-point control scheme. Consumers are guaranteed a minimal pressure difference $\Delta p_{\min}$ between supply and return

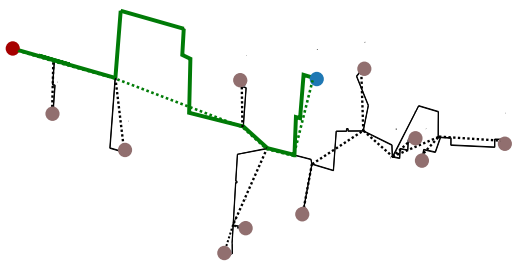

Fig. 1: Structure of example network. Dashed lines show the model after reduction. The critical path from the power plant (red circle) and worst point (blue circle) is indicated in green. All other demands are shown as grey circles.

to ensure the flow through their heat exchanger station [13]. The worst-point is defined as the consumer (k,l) with the smallest pressure difference, e.g. $\Delta p_{kl} \leq \Delta p_{ij} \ \forall (i,j) \in \boldsymbol{E}^{demand}$. The pressure at the heating plant is actively controlled such that the worst-point pressure difference exactly matches $\Delta p_{\min}$, i.e., for the wort-point edege (k,l) we have

$$p_k = p_{set}, \qquad p_l = p_{set} - \Delta p_{\min}, \tag{11}$$

where p_{set} is a reference pressure defined by the network operator. We assume that the worst-point edge is known in advance as is commonly the case in today's networks. Note that fixing the pressure at the worst-point reflects current practice in many district heating networks. However, our approach would work equally well if the pressure is fixed at any other point, e.g., the heating plant, or by another logic.

The functional relations (1) - (11) form a system of nonlinear equations. To simplify our notation we summarise this as a mapping $(\boldsymbol{y}, \boldsymbol{\theta}, \boldsymbol{\eta}) \mapsto \boldsymbol{e}(\boldsymbol{y}, \boldsymbol{\theta}, \boldsymbol{\eta})$ which couples the demand $\boldsymbol{\theta} := (Q_{ij}),\ \forall (i,j) \in \boldsymbol{E}^{demand}$ with the network state $\boldsymbol{y} := (p_i, T_i, T_{kl}^{\text{end}}, T_{kl}^{\text{start}}, \dot{m}_{kl}),\ \forall i \in \boldsymbol{V}, (k,l) \in \boldsymbol{E}$ and set point values $\boldsymbol{\eta} := (p_{set}, \Delta p_{\min}, T_{ij}^{\text{set}}),\ \forall (i,j) \in \boldsymbol{E}^{demand} \cup \boldsymbol{E}^{heating}$ and postulate

$$\boldsymbol{e}(\boldsymbol{y}, \boldsymbol{\theta}, \boldsymbol{\eta}) = 0. \tag{12}$$

The proof of uniqueness and existence of the solution can be done analogous to [2].

III. Model Reduction

A first step to reduce the complexity of (12) is to summarise pipes in a line, see Fig. 1. More specifically, we consider paths of maximal length consisting only of pipes and bends with the same pipe properties and no intersections, loads or generators at internal nodes. The set of all edges lying on such a path from i to j is denoted as $\boldsymbol{P_{ij}}$. The set of all such paths is $\boldsymbol{P}$. Every pipe and bend will be associated with exactly one path. For the network equations (12) we then consider new edges E_{ij}^P for each path $\boldsymbol{P_{ij}}$. The edge E_{ij}^P has the same values for d_{ij} and λ_{ij} as the pipes within $\boldsymbol{P_{ij}}$. The length l_{ij} results from adding up the lengths of all pipes on their path,

$$l_{ij} = \Sigma_{(k,l) \in \boldsymbol{P_{ij}}} l_{kl}. \tag{13}$$

The temperature T_{ij}^{end} of edge E_{ij}^{P} is given by (4) with length (13). The pressure loss Δp_{ij} is determined by expanding (5) with an additional constant bend friction factor $f_{B,ij}$. It approximates the influence of bends on overall pressure losses on a path. The factor $f_{B,ij}$ is calculated by solving (5) and (7) for all elements (k,l) on $\boldsymbol{P_{ij}}$ for the nominal mass flow rate $\dot{m}_{nom}$ [14]. We then divide the accumulated total pressure loss by the pressure loss due to pipes only. We get

$$\Delta p_{ij} = f_{B,ij}\, f_{\mathrm{D},ij}\, \frac{8 l_{ij}}{\pi^2 \rho d_{ij}^5}\, \dot{m}_{ij} |\dot{m}_{ij}|, \tag{14}$$

with

$$f_{B,ij} = \frac{\Sigma_{(k,l)\in \boldsymbol{P_{ij}}} \Delta\, p_{kl}(\dot{m}_{nom})}{\Sigma_{(k,l)\in \boldsymbol{P_{ij}} \cap \boldsymbol{E}^{pipe}} \Delta\, p_{kl}(\dot{m}_{nom})}. \tag{15}$$

We solve (12) for the reduced graph $G' = (\boldsymbol{V}', \boldsymbol{E}')$ with $\boldsymbol{E}' = \boldsymbol{E}^{demand} \cup \boldsymbol{E}^{heating} \cup \boldsymbol{E}^{P}$ where $\boldsymbol{E}^{P}$ is the set of all such edges E_{ij}^{P} and $\boldsymbol{V}' \subseteq \boldsymbol{V}$ is the set of nodes that are the start or end of any edge in $\boldsymbol{E}'$. Using the simplifications described in (13) – (15) the mapping $\boldsymbol{e}(\boldsymbol{y}, \boldsymbol{\theta}, \boldsymbol{\eta})$ is thereby reduced to the mapping $\bar{\boldsymbol{e}}(\boldsymbol{y}', \boldsymbol{\theta}, \boldsymbol{\eta})$ with $\boldsymbol{y}' = (p_i,\, T_i,\, T_{kl}^{\text{end}},\, T_{kl}^{\text{start}},\, \dot{m}_{kl}), \forall i \in \boldsymbol{V}', (k,l) \in \boldsymbol{E}'$.

Our second approach to reduce model complexity is to simplify equation (14) that contains the Darcy friction factor $f_{D,ij}$ which is complex to compute. Instead of adapting it to the current mass flow, we fix it to its value $f_{D,ij,nom}$ at the nominal mass flow $\dot{m}_{nom}$. This way, all coefficients can be precomputed and the pressure loss includes quadratic equations only, leading to the mapping $\tilde{\boldsymbol{e}}(\boldsymbol{y}', \boldsymbol{\theta}, \boldsymbol{\eta})$.

IV. State Estimation and Linearisation

Fixing the set point values $\boldsymbol{\eta}$, equations $\boldsymbol{e}(\boldsymbol{y}, \boldsymbol{\theta}, \boldsymbol{\eta}) = 0$ allows to define a mapping

$$\boldsymbol{y} = \boldsymbol{h}(\boldsymbol{\theta}). \tag{16}$$

It has the meaning of a state estimator since it outputs the system state given demand measurements or estimates.

The estimator is now extended to yield uncertainties as well. To this end, we assume that the demand follows a normal distribution $\boldsymbol{\theta} \sim \boldsymbol{N}(\boldsymbol{\theta}_0, \Sigma_{\boldsymbol{\theta}})$ with expected demands $\boldsymbol{\theta}_0$ and covariance matrix $\Sigma_{\boldsymbol{\theta}}$. We approximate the state estimation by its first order Taylor series around the expected demand

$$\boldsymbol{y} \approx \boldsymbol{y}^{lin} = \boldsymbol{h}(\boldsymbol{\theta}_0) + \boldsymbol{J}_{\boldsymbol{\theta}_0}(\boldsymbol{\theta} - \boldsymbol{\theta}_0), \tag{17}$$

where the Jacobian matrix $\boldsymbol{J}_{\boldsymbol{\theta}_0}$ is calculated by the implicit function theorem:

$$\boldsymbol{J}_{\boldsymbol{\theta}_0} \coloneqq \left.\frac{\partial\, \boldsymbol{h}}{\partial\, \boldsymbol{\theta}}\right|_{\boldsymbol{\theta}=\boldsymbol{\theta}_0} = -\left[\frac{\partial \boldsymbol{e}\big(\,\boldsymbol{y}, \boldsymbol{\theta}_0, \boldsymbol{\eta}\big)}{\partial\, \boldsymbol{y}}\right]^{-1} \frac{\partial \boldsymbol{e}\big(\,\boldsymbol{y}, \boldsymbol{\theta}_0, \boldsymbol{\eta}\big)}{\partial\, \boldsymbol{\theta}}. \tag{18}$$

Applying (17) to normally distributed demands we obtain estimated states that follow a multivariate normal distribution $\boldsymbol{y}^{lin} \sim \boldsymbol{N}(\boldsymbol{y}_0, \Sigma_{\boldsymbol{y}})$ whose parameters are given as

$$\boldsymbol{y}_0 = \boldsymbol{h}(\boldsymbol{\theta}_0), \tag{19}$$

$$\Sigma_{\boldsymbol{y}} = \boldsymbol{J}_{\boldsymbol{\theta}_0}\, \Sigma_{\boldsymbol{\theta}}\, \boldsymbol{J}_{\boldsymbol{\theta}_0}{}^{T}. \tag{20}$$

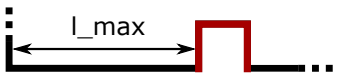

Fig. 2: Stretching arc with maximal pipe length l_{max}.

The same can be done for the simplified mappings $\bar{\boldsymbol{e}}$ and $\tilde{\boldsymbol{e}}$ to estimate $\boldsymbol{y}'$.

V. Numerical Evaluation

We evaluate the proposed approach for model reduction and state estimation based on the network shown in Fig. 1 which is a part of a real district heating network, modified to ensure privacy.

A. Verification of Model reduction

To release mechanical tensions due to thermal expansion, stretching arcs need to be installed in long, straight pipe sections, see Fig. 2. The maximal pipe length l_{max} without a stretching arc is given by the manufacturers [14]. Such a cascade of four bends and a pipe of maximal length serves as the test case for our investigation of the accuracy of the loss approximation for path segments. We evaluate the accuracy of using aggregation factor f_B as well as using both f_B and a constant $f_{D,nom}$. We examine this for pipes from a nominal diameter of $20\,mm$ (DN20) to $400\,mm$ (DN400) at typical temperatures of $65\,^\circ C$ and $110\,^\circ C$ for mass flows between 0 and the maximal recommended mass flow rate $\dot{m}_{max}$ given by [14].

As Fig. 3a shows, the error due to the usage of f_B remains close to zero over the whole operating range. The biggest absolute deviations in pressure loss occurs in pipes of type DN400 for $\dot{m} = \dot{m}_{max} = 319.4\,kg/s$ and $T = 65\,^\circ C$. Without any simplifications the pressure loss for this case is $\Delta p = 295.6\,mbar$, the deviation due to simplifications is $0,4\,mbar\,(0,14\,\%)$.
Using a constant pipe friction factor $f_{D,nom}$ accounts for additional deviations in pressure losses, see Fig. 3b, which reach their peak at $4,7\,mbar\,(1,59\,\%)$ for $\dot{m} = \dot{m}_{max}$.

We evaluate an upper barrier for the model error due to model reduction by adding the maximal errors for all $\boldsymbol{P_{ij}}$ on the supply and return side lying between the feed-in and the worst-point discussed in Section II. The mass flows $\dot{m}_{ij}$ are adjusted for each $\boldsymbol{P_{ij}}$ individually in order to yield the maximum deviation. The summarising of edges as discussed in section III accounts for a maximum error of $0.54\,mbar$ at an overall diferential pressure of $934\,mbar$ which is a deviation of $0.058\,\%$. Usage of both a constant f_B and $f_{D,nom}$ accounts for a maximum error of $17.8\,mbar$ at a diferential pressure of $469\,mbar$ which corresponds to a deviation of $3.8\,\%$.

Merging the elements on paths $\boldsymbol{P}$ leads to a significant reduction of network elements. For our test network the number of nodes is reduced from 267 to 48, the number of edges from 277 to 58, cf. Fig. 1.

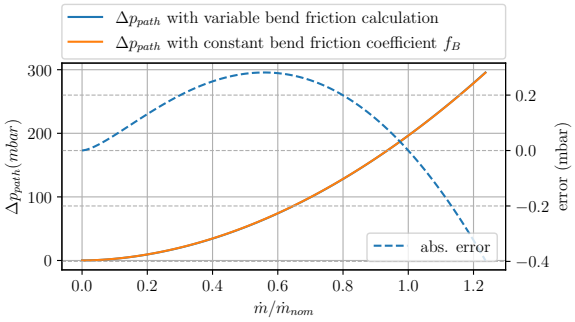

(a) Straight pipe with stretching arc with detailed modeling of bends and with use of f_B.

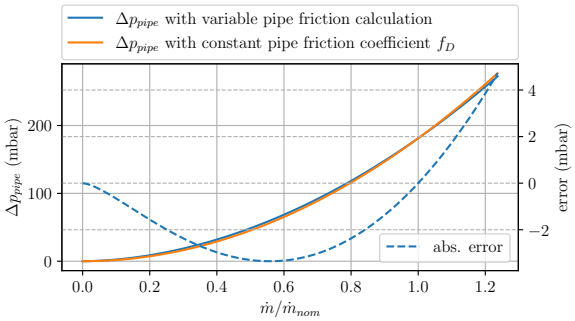

(b) Straight pipe of length l_{max} with variable and constant f_D.

Fig. 3: Pressure losses in a pipe of type DN400 with different model reduction methods.

B. Linearised Probabilistic State Estimation

We apply the procedure laid out in Section IV on the reduced model $\bar{\boldsymbol{e}}$ which incorporates the reduced bend representation and a non-constant Darcy friction factor. The parameters for the demand distribution $\boldsymbol{\theta} \sim \boldsymbol{N}(\boldsymbol{\theta}_0, \Sigma_{\boldsymbol{\theta}})$ are estimated based on historical demands. The consumption mean vector $\theta_{0,i} = \frac{1}{24}\frac{1}{D}\sum_{h=1}^{24}\sum_{d=1}^{D}\dot{Q}_i^{d,h}$ is given by averaging the hourly mean consumption $\dot{Q}_i^{d,h}$ for each consumer i at hour h of day d.

The entries of the covariance matrix $\Sigma_{\boldsymbol{\theta}} = \left(\Sigma_{\boldsymbol{\theta}}^{ij}\right)$ are gathered independently for each hour and averaged afterwards in order to receive a reasonable correlation structure but also avoiding too large variances. This leads to $\Sigma_{\boldsymbol{\theta}}^{ij} = \left(\frac{1}{24}\right)^3 \sum_h \sigma_i^h \sum_h \sigma_j^h \sum_h \rho_{ij}^h$, with σ_i^h and ρ_{ij}^h being the standard deviation and the normalised cross-correlation for the historical demands of the consumer i respectively j at hour h.

Let $\hat{\boldsymbol{y}}^{\text{lin}} \sim \boldsymbol{N}(\hat{\boldsymbol{y}}_0, \Sigma_{\boldsymbol{y}})$ denote the state estimated by (17) given this demand distribution. We approximate the real network state distribution $\boldsymbol{y}^{\text{MC}}$ by drawing $N = 50000$ independent sample demands out of the demand distribution and solve (16) with the full model $\boldsymbol{e}$ for each sample using the Newton-Raphson method. Samples for which at least one entry in $\boldsymbol{\theta}$ is negative are discarded in this process, since negative demands are not physically feasible.

We evaluate the performance of our approach based on the marginal distributions $\hat{y}_k^{lin} \sim N\left(\hat{y}_0^k, \hat{\Sigma}_{\boldsymbol{y}}^{k,k}\right)$ for each state variable k. Since the uncertainties predicted by the linearised model are normally distributed but approximately 2% of the samples are discarded during the Monte Carlo Sampling, the prediction will always deviate from the sampled state. In order to yield a fair evaluation the results are compared against an one dimensional normal distribution $y_k^{fit} \sim N\left(y_0^k, {\sigma_y^k}^2\right)$ where y_0^k and $(\sigma_y^k)^2$ are the mean and the standard deviation of the sampled results for the variable k.

TABLE I: Deviations between the predicted distribution parameters and the sample's mean and standard deviation.

		MAE	$MAPE$	$RMSE$	$RMSPE$
$\dot{m}$	mean	$0.017\,kg/s$	$0.64\,\%$	$0.025\,kg/s$	$0.77\,\%$
	std.	$0.013\,kg/s$	$2.10\,\%$	$0.021\,kg/s$	$2.34\,\%$
p	mean	$0.906\,mbar$	$0.02\,\%$	$0.987\,mbar$	$0.02\,\%$
	std.	$0.179\,mbar$	$1.12\,\%$	$0.201\,mbar$	$1.21\,\%$
T	mean	$0.090\,°C$	$0.09\,\%$	$0.176\,°C$	$0.18\,\%$
	std.	$0.151\,°C$	$17.0\,\%$	$0.332\,°C$	$25.5\,\%$

Table I lists the Mean-Absolute-Error (MAE) and the Root-Mean-Squared-Error ($RMSE$) as well as the Mean-Absolute-Percentage-Error ($MAPE$) and the Root-Mean-Squared-Percentage-Error ($RMSPE$) between the edistribution parameters estimated by the linearised model and the parameters based on the sampled results.

Fig. 5 shows exemplary the estimated and the sampled mass flows at the heating plant as well as the temperature at the supply of the demand which is the furthest to the right and therefore the furthest away from the heating plant.

We scale the state variables such that $\hat{y}_k^{lin}$ has a unit variance and zero mean, i.e., for each sample y_k^i we consider the scaled sample $\overline{y}_k^i = \frac{y_k^i - \hat{y}_{k,0}}{\hat{\Sigma}_{\boldsymbol{y}}^{k,k}}$. Fig. 4 shows the cumulated distribution function (cdf) for the scaled state variables.

The sampled distributions for mass flows and pressures match well with the predicted ones, whereas the distribution for temperatures shows significant deviations. The temperature T_{ij}^{end} is limited by the temperature at the start of the edge T_{ij}^{start} and the soil temperature T_a, cf. (4). The temperature with the highest probability is close to T_{ij}^{start}. However significantly lower temperatures can occur if $\dot{m}_{ij}$ is small. This leads to a left skewed distribution over the real temperatures.

VI. Conclusion

In this paper we considered approaches to reduce the computational burden for estimating the state variables of a district heating network as well as uncertainties for these variables. We showed that the pressure losses due to bends and friction in the pipes can be merged into one pressure loss equation using aggregated edges and a correction factor. This approach reduces the number of edges in the network by approximately $80\,\%$ and significantly decreases the computational burden. Further reduction was achieved by fixing the Darcy friction factor onto a constant value, leading to slightly higher calculation errors compared to the approach mentioned beforehand. Both simplifications are considered to be valid approaches for model reduction in district heating.

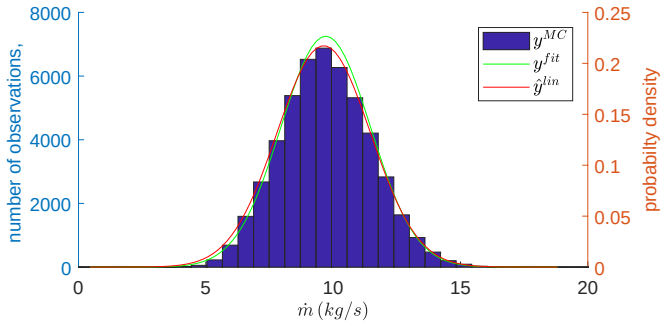

(a) Mass flow at the heating plant.

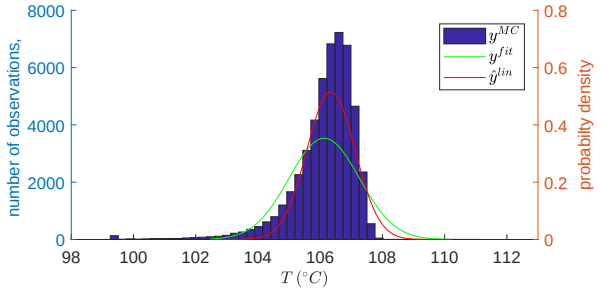

(b) Temperature at the supply node at the demand furthest to the right.

Fig. 5: Comparison of the estimated marginal distribution in red and the sampled distribution in blue. The green line shows a normal distribution with the samples mean and variance.

We proposed a method to estimate normally distributed uncertainties for the state variables given normal distributed demand uncertainties, using a local linearisation of the state equations. Compared to Monte Carlo sampling baseline the mean deviation for the expected values of the network state is below 1% for the predicted distribution. For pressure and mass flow standard deviations are estimated within a single digit percentage error margin. The prediction errors are larger for the temperature whose real distribution is strongly left skewed due to the way the temperature is restricted. In a heating grid low temperatures are associated with low mass flows and therefore low heat demand. This indicates that the situations with high error are uncritical network states in which the deviations seem less significant.

Acknowledgment

We thank Alexander Matei for helping to develop the model as well as the members of the project EnEff:Wärme MeFlexWärme for the constructive discussions.

References

[1] Henrik Lund, Sven Werner, Robin Wiltshire, Svend Svendsen, Jan Eric Thorsen, Frede Hvelplund, and Brian Vad Mathiesen. 4th generation district heating (4gdh): Integrating smart thermal grids into future sustainable energy systems. *Energy*, 68:1–11, 2014.

[2] Tingting Fang and Risto Lahdelma. State estimation of district heating network based on customer measurements. *Applied Thermal Engineering*, 73(1):1211–1221, 2014.

[3] Xuezhi Liu, Jianzhong Wu, Nick Jenkins, and Audrius Bagdanavicius. Combined analysis of electricity and heat networks. *Applied Energy*, 162:1238–1250, 2016.

[4] Ilyes Ben Hassine and Ursula Eicker. Impact of load structure variation and solar thermal energy integration on an existing district heating network. *Applied Thermal Engineering*, 50(2):1437–1446, 2013.

[5] Jean Duquette, Andrew Rowe, and Peter Wild. Thermal performance of a steady state physical pipe model for simulating district heating grids with variable flow. *Applied Energy*, 178:383–393, 2016.

[6] Guoqiang Sun, Wenxue Wang, Yi Wu, Wei Hu, Zijun Yang, Zhinong Wei, Haixiang Zang, and Sheng Chen. A nonlinear analytical algorithm for predicting the probabilistic mass flow of a radial district heating network. *Energies*, 12(7):1215, 2019.

[7] *Equivalent Models of District Heating Systems for On-line Minimization of Operational Costs of the Complete District Heating System*. 04 1999.

[8] Helge V Larsen, Benny Bøhm, and Michael Wigbels. A comparison of aggregated models for simulation and operational optimisation of district heating networks. *Energy Conversion and Management*, 45(7):1119–1139, 2004.

[9] Achim Loewen. *Entwicklung eines Verfahrens zur Aggregation komplexer Fernwärmenetze*. 04 2001.

[10] Michael Wetter, Marcus Fuchs, Pavel Grozman, L. Helsen, Filip Jorissen, Moritz Lauster, Dirk Mueller, Christoph Nytsch-Geusen, Damien Picard, and Matthis Thorade. Iea ebc annex 60 modelica library – an international collaboration to develop a free open-source model library for buildings and community energy systems. page 395–402, 12 2015.

[11] C F Colebrook. Turbulent flow in pipes, with particular reference to the transition region between the smooth and the rough pipe laws. *Journal of the Institution of Civil Engineers*, 11(4):133–156, February 1939.

[12] I. E. Idelchik. Handbook of Hydraulic Resistance, 2nd Edition. *Journal of Pressure Vessel Technology*, 109(2):260–261, May 1987.

[13] ENTEGA AG, Darmstadt, Germany. *Technische Anschlussbedingungen (TAB) Fernwärme Darmstadt*, 2017.

[14] isoplus Fernwärmetechnik Vertriebsgesellschaft mbH, Rosenheim, Deutschland. *Starre Verbundsysteme*, 2011.

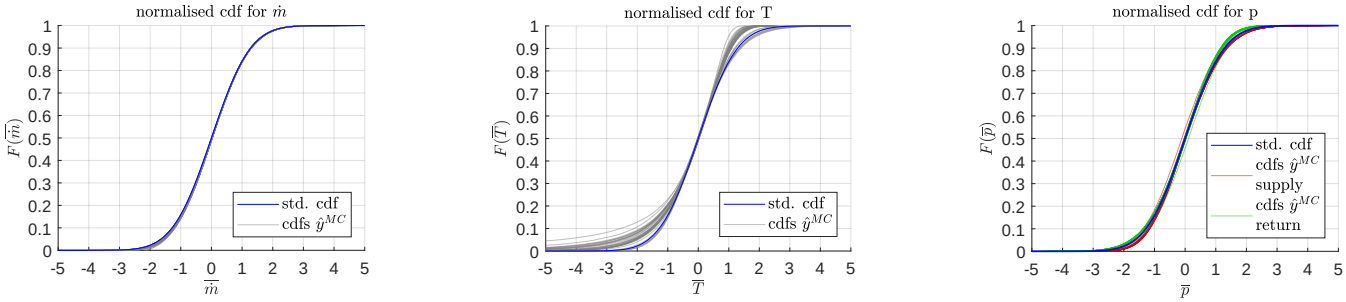

(a) mass flows (b) temperature (c) pressures

Fig. 4: Marginal cumulative distribution functions of $\boldsymbol{y}^{\mathrm{MC}}$ (gray lines). The horizontal axis is scaled such that the predicted distribution $\hat{\boldsymbol{y}}^{\mathrm{lin}}$ has unit variance. If $\boldsymbol{y}^{\mathrm{MC}}$ matches $\hat{\boldsymbol{y}}^{\mathrm{lin}}$ the blue line will result.